



Effect of ammonium bisulphite and chloride on the pitting and stress corrosion cracking resistance of super duplex stainless steel pipes under combined internal pressure and axial tension

Journal:	<i>Materials and Corrosion</i>
Manuscript ID	maco.201810502.R3
Wiley - Manuscript type:	Article
Date Submitted by the Author:	n/a
Complete List of Authors:	Lasebikan, Daley; University of Aberdeen, Engineering Akisanya, Alfred; University of Aberdeen, Engineering Deans, Bill; University of Aberdeen, Engineering
Keywords:	Ammonium bisulphite, Chloride, Combined loading, Super Duplex Stainless Steel, Mini pipe

SCHOLARONE™
Manuscripts

1
2
3 Effect of ammonium bisulphite and chloride on the pitting and stress corrosion cracking
4 resistance of super duplex stainless steel pipes under combined internal pressure and axial
5
6
7
8 tension
9
10

11
12 B. A. Lasebikan*, A. R. Akisanya and W.F. Deans
13

14 School of Engineering, University of Aberdeen, Aberdeen AB24 3UE, U.K.
15
16
17

18 **Keywords:**

19 Ammonium bisulphite, chloride, super duplex stainless steel, pitting, crack initiation, stress
20 corrosion cracking, combined loading, axial tension, internal pressure, mini pipe.
21
22
23
24
25

26 **ABSTRACT**

27 Combined loading of axial tension and internal pressure on the corrosion resistance of SDSS
28 pipes at 90 °C in ammonium bisulphite - 3.5 wt% NaCl environment was examined. The
29
30 additions of ammonium bisulphite up to 1000 ppmw increased the corrosion potential and
31
32 decreased the pitting resistance. The optimum concentration for maximum resistance of the
33
34 SDSS pipe under the various load conditions is 100 ppmw ammonium bisulphite. When an
35
36 internal pressure less than the nominal burst pressure at 90 °C was applied, crack initiation
37
38 from pits was observed in pipes subject to internal pressure and combined loading, while no
39
40 cracks was observed in nominally identical pipes subject to only axial tension. Qualification
41
42 (corrosion) tests in relevant environments are usually from samples subject to single mode
43
44 loading. However, in service an understanding of the relationship between service stresses
45
46 caused by load and pressure and the ability of the material to resist crack initiation is
47
48 required. Therefore, the use of mini pipes is proposed to better define application limits in
49
50
51
52
53
54
55

56 _____
57 * Corresponding Author: daley.lasebikan@bp.com
58
59
60

1
2
3 corrosive environments once the failure envelope is determined in the absence of any
4
5 corrosive environment.
6
7
8
9

10 **1 INTRODUCTION**

11 Duplex and super duplex stainless steel pipes are used extensively in the oil and gas and
12
13 chemical process industry because of their relatively high strength and corrosion resistance
14
15 compared to many low alloy steels. This is particularly the case in oil and gas wells
16
17 operating at High Pressure and High Temperature (HPHT) where the high tensile strength of
18
19 super duplex stainless steel (SDSS) enables the use of thinner wall pipe resulting in weight
20
21 and cost savings. DSS and SDSS has a dual phase microstructure containing γ - austenite
22
23 (face centered cubic) and α - ferrite (body centered cubic) with approximate equal volume
24
25 fraction. The microstructure and corrosion resistance are achieved by control of chemical
26
27 composition, heat treatment cycle and coldworked for high strength. Due to the development
28
29 of a thin protective oxide layer, SDSS are normally passive in corrosive environments that
30
31 may contain, for example, CO_2 , H_2S , and other sulphur containing species like ammonium
32
33 bisulphite. However, such passive films are often susceptible to localised breakdown
34
35 resulting in dissolution of the underlying metal by pitting that may subsequently act as
36
37 initiation sites for cracks [1, 2].
38
39
40
41
42
43
44
45

46 One of the important factors for effective use of corrosion resistant alloys is the
47
48 understanding of the effects of environmental and metallurgical variables on the general and
49
50 localised corrosion (e.g. pitting) behaviour and on the resistance to environment assisted
51
52 cracking (EAC). EAC may originate from either H_2S enhanced hydrogen absorption or H_2S
53
54 enhanced breakdown of the passive oxide film by synergistic action between chloride and
55
56
57
58
59
60

1
2
3 H₂S. The H₂S content and salinity of the aqueous phase are critical variables affecting EAC
4 susceptibility in the production environment [3-6]. Past failures of cold worked DSS [7, 8]
5 and SDSS [9] tubulars used in oil and gas wells clearly demonstrate that the physical
6 understanding of EAC remains incomplete despite extensive research on the subject over
7 many decades.
8
9

10
11
12
13
14
15
16
17 A typical completion system for an oil and gas well is made up of concentric tubulars, see
18 Figure 1. The production tubular, which transports the hydrocarbon from the production zone
19 to the wellhead, is sometimes made of DSS or SDSS depending on the CO₂ and H₂S content
20 of the hydrocarbon. Specialised cement is used to isolate the production casing from the
21 surrounding formation and to provide structural integrity. The production annulus, i.e. the
22 space between the production tubing and production casing (annulus A in Figure 1) normally
23 contains brine (e.g. CaCl₂, NaCl, NaCl/NaBr, CaCl₂/CaBr₂ etc.) and/or treated water
24 (deionised, seawater etc.) to provide hydrostatic head against the ingress of any well fluids
25 through the packer that seals the void between the production tubing and production casing
26 just above the liner. The brine or water is treated using sodium bisulphite (NaHSO₃) or
27 ammonium bisulphite (NH₄HSO₃) to reduce oxygen corrosion to negligible levels.
28
29 Ammonium bisulphite is the main oxygen scavenger used in the annulus fluid. Experience
30 has shown that brine that contains less than 10 ppbw (part per billion by weight) of dissolved
31 oxygen is deaerated and therefore not corrosive to the carbon steel casing and production
32 tubing [10]. The effectiveness of ammonium bisulphite as oxygen scavenger is presented
33 elsewhere [11]. Ammonium bisulphite has been implicated in the corrosion related failure of
34 production tubular used in a few HPHT wells [8, 9]. Thus, material selection for production
35
36
37
38
39
40
41
42
43
44
45
46
47
48
49
50
51
52
53
54
55
56
57
58
59
60

1
2
3 tubulars in well completion requires an understanding of the relationship between service
4 stresses and the ability of the material to resist crack initiation in the service environment. In
5
6
7
8 HPHT wells axial load is limited (weight of tubing string) and internal pressure is dominant.
9

10
11
12 Most of the published research to-date on pitting and stress corrosion cracking are based on
13 single mode or uniaxial loading of the material in CO₂/H₂S or chloride environment. Test
14
15 results from four-point bend specimens of austenitic stainless steel in chloride environment
16
17 showed increased susceptibility to pitting corrosion with increased pre-existing surface
18
19 roughness or damage [12] while compact tension test results in simulated boiling water
20
21 reactor conditions showed that ppb level of chloride may result in fast stress corrosion
22
23 cracking of low alloy steels [13]. Stress corrosion cracking of 22Cr and 25Cr SDSS under
24
25 evaporative seawater conditions using uniaxial tensile specimen has been shown to depend
26
27 on the level of applied stress and the test temperature; as the applied stress increased the
28
29 threshold temperature for corrosion and cracking decreased [14]. A summary of the effects
30
31 of intrinsic material parameters (e.g. chemical composition, microstructure and surface
32
33 condition) and environment (e.g. pH, temperature, concentration of aggressive species and
34
35 dissolved oxygen) on the initiation and growth of pits in metals has recently been presented
36
37 by Soltis [15]. Although Keitelman and Alvarez elucidation of the localised acidification
38
39 pitting model (initiation and growth) by Galvele stated that it did not consider the
40
41 interactions between dissolved metal ions and chloride or other anionic species in solution;
42
43 they concluded that laboratory experiments and field experience with alloys like 22Cr and
44
45
46
47
48
49
50
51
52
53
54
55
56
57
58
59
60
25Cr SDSS confirmed quantitatively the predictions of Galvele's model [16]. The main point

1
2
3 of the mechanism is that localised pH drop on the anode surface is necessary to sustain
4
5 pitting.
6
7
8
9

10 Unlike corrosion in chloride environment and H₂S, there has been limited study of corrosion
11
12 in sulphite environment. Hornlund et al. [17] examined the diffusion of hydrogen during
13
14 cathodic protection of carbon steel in a solution of NaCl with added sulphite. The authors are
15
16 not aware of any previous study of the corrosion of SDSS tubulars subject to combined
17
18 loading of axial tension and internal pressure in ammonium bisulphite-brine environment.
19
20 Practical situations are closer to combined loading unlike single mode loading typically used
21
22 for corrosion / material tests. For example, the C ring test sample simulate the
23
24 circumferential stresses induced on the tubing by internal pressure (hoop stress) where bent
25
26 beam and constant load tests are performed to reproduce longitudinal stresses induced by the
27
28 weight of the production tubing string in a well completion. The aim of the current study is
29
30 to assess the pitting corrosion behaviour and the susceptibility to stress corrosion cracking
31
32 (SCC) under combined loading (axial tension and internal pressure) of SDSS pipes in
33
34 ammonium bisulphite-chloride environment without the presence of CO₂ or H₂S. The results
35
36 of the corrosion tests would provide a better assessment of the effect of ammonium
37
38 bisulphite on corrosion resistance and behaviour of SDSS pipes in a well completion
39
40 production annulus that is nominally free of CO₂ or H₂S.
41
42
43
44
45
46
47
48

49 **2 EXPERIMENTAL PROCEDURES**

50 51 **2.1 Material and specimen preparation**

52 A 25Cr SDSS with the element composition shown in Table 1 was considered and Figure 2
53
54 illustrates the normal microstructure in the longitudinal (rolling) and transverse direction of
55
56
57
58
59
60

1
2
3 the SDSS as received Sumitomo pipes from a well completion. The ferrite and austenite ratio
4 were 49% and 51% respectively. The mechanical properties of the material are presented
5 elsewhere [18]. For completeness, the effects of temperature on the Young's modulus, yield
6 strength and the ultimate tensile strength of the material are shown in Table 2. The element
7 composition in Table 1 indicates the material has a Pitting Resistance Equivalent Number
8 (PREN₃₂) of 45 for the PREN formula in equation. PREN is a measure of the intrinsic
9 resistance of a material to pitting corrosion and is determined from the element composition
10 (in percentage weight) of the material [19]:
11
12
13
14
15
16
17
18
19
20
21
22
23

$$24 \quad \text{PREN}_a = \text{Cr} + 3.3 \text{ Mo} + a \text{ N} \quad (1)$$

25
26 where “*a*” is a constant that ranges from 16 to 32.
27
28
29
30

31 Mini pipe samples were machined from the parent tubing of the SDSS along the longitudinal
32 rolling direction. Airao et al. found that surface finish obtained in wet machining of SDSS
33 were much better compared to dry machining [20]. Coolant was used for all cutting and
34 machining processes to minimise the effect of the heat associated with the machine on the
35 mechanical properties and SDSS microstructure and ensure a good surface finish. The mini
36 pipes (Figure 3) have an outside diameter of 8 mm, wall thickness of 0.25 mm ± 0.2 µm
37 (tolerance) and a gauge length of 25 mm including 2.5 mm thick section (spanner flat) before
38 the treads to facilitate fastening to fixtures prior to application of the epoxy resin (Figure 4).
39
40 The surface of the pipe was mechanically polished in the hoop direction by using a P360 grit
41 and subsequently using a P600 grit (30 µm). The surface was then cleaned with acetone.
42
43
44
45
46
47
48
49
50
51
52
53
54
55
56
57
58
59
60

1
2
3 Titanium wire inserted in a 1 mm diameter shrink sleeve was spot welded to one end of the
4 mini pipe to facilitate current measurement during corrosion test. The pipes were then
5 connected to ceramic adaptors (Manufactured by Dynamic Ceramic, Crewe Hall Enterprise
6 Park, Weston Road, Crewe, CW1 6UA, UK) as shown in Figure 4. To avoid crevice
7 corrosion, the areas of the pipe near the connection ends were covered in epoxy resin (two-
8 pack araldite) leaving an exposure surface area of 6 cm² in the gauge section (see Figure 4).
9
10
11
12
13
14
15
16
17

18 **2.2 Test Environment**

19 The solutions used in the corrosion tests were 0.1, 1 and 3.5 wt% NaCl plus various
20 concentration of ammonium bisulphite (0, 100, 500 and 1000 ppmw). Here and thereafter the
21 unit ppm (part per million) for the concentration of ammonium bisulphite is in weight. Each
22 test solution was made with analytical grade NaCl in deionised water plus additions of
23 various concentration of ammonium bisulphite. The pH and dissolved oxygen (DO) of the
24 solution were measured at room temperature using electrodes and DO probe supplied by
25 Fisher Scientific. Table 3 shows the pH and DO of the various solutions prior to heating the
26 solution to the test temperature of 90 °C.
27
28
29
30
31
32
33
34
35
36
37
38
39

40 **2.3 Corrosion tests**

41 Critical Pitting Temperature (CPT)

42 ASTM G48 [21] test method is widely used to determine the pitting resistance of corrosion
43 resistant alloys (CRAs) in a standard environment and can provide useful information
44 regarding the susceptibility of specific materials to pitting. The procedure involves the
45 immersion of the sample in the test environment at the temperature of interest for 72 hours.
46 The sample is then examined under an optical microscope to detect the presence of pits. If
47 pits are not detected the procedure is repeated at an increased temperature until pits are
48
49
50
51
52
53
54
55
56
57
58
59
60

1
2
3 detected in the sample. This temperature is taken as the CPT. Thus, CPT is the maximum
4 temperature below which no pitting corrosion is expected and above which pitting corrosion
5 is highly likely to occur when the material is exposed to the test environment.
6
7
8
9

10
11
12 Immersion test in Ferric chloride environment was carried out on a sample removed from the
13 7” cold worked SDSS tubing under consideration according to ASTM G48 standard method
14 E [21] described above; this test gave a CPT value of 85 °C. CPT of Hot Isostatic pressed
15 (manufactured) SDSS 32707 in 3.5 wt% NaCl solution investigated by Xu et al. in
16 potentiodynamic corrosion tests measured between 55 and 65 °C [22]. However, the CPT of
17 SDSS was determined in 6% Ferric Chloride according to the ASTM G48 tests at 80 °C by
18 another researcher [23]. Thus, potentiodynamic corrosion tests (described below) were
19 carried out at 90 °C.
20
21
22
23
24
25
26
27
28
29
30

31 32 33 Potentiodynamic Corrosion Tests 34

35 The corrosion tests in this study were based on potentiodynamic polarisation technique [24]
36 which can provide useful information regarding the susceptibility of specific materials to
37 corrosion in a particular environment. The tests were carried out in a purposely-designed and
38 manufactured HPHT autoclave [25]. The autoclave was filled with the test solution (i.e. the
39 electrolyte) and an electrochemical cell consisting of four electrodes was made up as
40 illustrated in Figure 5. The volume of the solution used was 1000 ml; this is consistent with
41 the recommended minimum 100 ml per square centimetre of the exposed surface area of the
42 mini pipe which was 6 cm² [26]. The reference electrode (RE) used in all the experiment was
43 a silver|silver-chloride (Ag|AgCl) half cell (supplied by Fisher Scientific) in a 3.5M
44
45
46
47
48
49
50
51
52
53
54
55
56
57
58
59
60

1
2
3 potassium chloride (KCl) solution; the reference electrode was used to monitor and maintain
4 the potential at the surface of the working electrode (WE). The SDSS mini pipe was the WE
5
6
7 whilst two graphite rods were used as counter electrodes (AUX).
8
9

10
11
12 The four electrodes were connected to a computer-controlled potentiostat (Princeton Applied
13 Research Model 263A Potentiostat/Galvanostat). The potential of the working electrode was
14
15 varied at a selected rate by the application of a current through the electrolyte and the
16
17 resulting current and potential between the WE and RE are monitored and recorded by a
18
19 potentiostat; the relationship between the current and potential is used to assess the onset of
20
21 pitting (breakdown of passivation) and repassivation.
22
23
24
25

26
27
28 The voltage and current in the electrochemical cell were continuously recorded using the
29
30 potentiostat in-built data logger. Using the computer-controlled potentiostat, the WE was
31
32 polarised in the noble direction from 25 mV below the open circuit potential (to minimise
33
34 cathodic polarisation and probable hydrogen adsorption) at a scan rate of 1 mV/s and
35
36 terminated at 0.5 mA. During anodic polarisation, the increase in potential of the mini pipe
37
38 results in loss of electrons. The scan rate must be slow enough to allow the rate determining
39
40 step of the overall reaction. Thus, the anodic dissolution rate in the various test environments
41
42 is a measure of the susceptibility of the pipe to pitting. The onset of pitting was determined
43
44 as the potential at which the recorded current density suddenly increased and exceeded 100
45
46 $\mu\text{A}/\text{cm}^2$ and did not fall below this value for 60 seconds. This approach was used to
47
48 determine the pitting potential, E_p , which provides a measure of the susceptibility of the
49
50 SDSS pipes to pitting in the ammonium bisulphite-chloride environment. The
51
52
53
54
55
56
57
58
59
60

1
2
3 potentiodynamic test was performed in duplicates to ensure tests were repeatable and
4
5 representative.
6
7

8
9
10 The electrical isolation of the mini pipes from the load fixtures using ceramic adaptors, the
11 use of earth-to-earth connection between the autoclave and potentiostat and the screening of
12 all the cables used for all connections (RE, WE, AUX and autoclave to potentiostat) ensured
13 adequate shielding and minimisation of noise and interference in the measured potential and
14 current.
15
16
17
18
19
20
21
22
23

24 Two sets of corrosion tests were performed at a temperature of 90 °C. First, the external
25 surface of the pipe at the gauge length was exposed to each test solution inside the autoclave
26 with no external mechanical loads applied to the pipes; this is referred to as the reference
27 test. A separate and second set of tests was carried out with axial tension and/or internal
28 pressure applied to the mini pipe while the external surface was exposed to the test solution
29 inside the autoclave. In both cases, the potentiostat was used to monitor and determine the
30 pitting potential as described above. Axial tension was applied in displacement control and at
31 a crosshead speed of 0.5 mm/min using a screw-driven Instron testing machine while the
32 internal pressure was applied using a hydraulic hand pump as described in [27]; the
33 pressuring medium was hydraulic oil.
34
35
36
37
38
39
40
41
42
43
44
45
46
47
48

49 Three load cases were considered: (i) an axial tension of 568 MPa which was within the
50 elastic limit based on the material properties at 90 °C (Table 2), (ii) an internal pressure of
51 48.3 MPa, which was 0.85 of the average measured burst pressure at 90 °C (and 0.72 of burst
52
53
54
55
56
57
58
59
60

1
2
3 pressure at room temperature), and (iii) a combined axial tension of 568 MPa and internal
4 pressure of 48.3 MPa. For the combined loading, the axial tension was first applied to the
5 mini pipe followed by the application of the internal pressure while the axial tension was
6 kept constant. In the absence of any corrosive environment, the experimentally measured
7 average burst pressure at 90 °C (without any externally applied axial load) was found to be
8 56.1 MPa, while failure under combined loading at 90 °C occurred at an internal pressure of
9 52 MPa and axial load of 665 MPa [27]. Thus, the chosen values of the axial load and
10 internal pressure for the current study are lower than those required for the failure of the pipe
11 in the absence of any corrosive environment as illustrated in Figure 6. This is important as
12 the purpose of the current study is to assess the susceptibility to pitting and pitting induced
13 failure in the pipes at loads that are below the nominal failure loads without the ammonium
14 bisulphite-chloride environment.
15
16
17
18
19
20
21
22
23
24
25
26
27
28
29
30
31
32

33 For each of the load cases, the autoclave containing the mini pipe was filled with the test
34 solution and solution heated to the test temperature using a heating jacket on the outer
35 surface of the autoclave. The pipes were left at open circuit condition during the heating
36 process until the test temperature of 90 °C was achieved (which took ~ 1 hour). Once the test
37 temperature was attained, the required load was applied in increment. When the load was
38 applied, the rupture of surface film on the specimen produces an immediate increase in
39 anodic current, which then decreases with time as repassivation occurs. Allowance was made
40 to ensure there was enough time for the stabilisation (~ 15 minutes) of OCP (open circuit
41 potential) before the corrosion test commenced by application of potential to the cell at a rate
42 of 1 mV/s. No specific attempt was made to ensure the test solution was oxygen free at the
43
44
45
46
47
48
49
50
51
52
53
54
55
56
57
58
59
60

1
2
3 test temperature, but small plastic hollow spheres were used to cover the 1000 ml solution to
4
5 minimise evaporation and ensure stable test temperature.
6
7

8 9 **2.4 Morphology of corrosion attack**

10 The external surface of the mini pipe samples after corrosion tests were cleaned before
11
12 examination. Optical microscope was used to investigate the presence of pits after the ASTM
13
14 G48 tests. A Hitachi S-520 scanning electron microscope (SEM) was used to examine
15
16 corrosion morphology on the external surface of the pipe after potentiodynamic polarisation
17
18 tests.
19
20
21
22
23

24 **3 RESULTS AND DISCUSSION**

25 **3.1 Critical pitting temperature (CPT)**

26 Immersion tests carried out according to the ASTM G48 standard method E [21] gave a CPT
27
28 of 85 °C for the SDSS pipe material considered in this study. Presence of pit was confirmed
29
30 by microscopic examination of one of the samples; this revealed pits of at least 25 µm wide
31
32 (Figure 7). The focus of the current study is the determination of the pitting potential in the
33
34 various chloride-ammonium bisulphite environments under combined load. Consequently,
35
36 no attempt was made in the current study to determine the phase where the pits were initiated
37
38 within the SDSS material. However, pitting corrosion study in chloride environment of 25Cr
39
40 SDSS similar to the material considered in the current study [28] and of DSS 2204 [29]
41
42 showed that pitting initiated from the austenite phase and the ferrite/austenite grain
43
44 boundary.
45
46
47
48
49
50
51

52 A number of researchers have found that the occurrence of pitting corrosion was an
53
54 important contributing factor in crack initiation during the process of SCC [13, 14 30].
55
56
57
58
59
60

1
2
3 Furthermore, many other researchers have shown that the temperature of maximum SCC
4 susceptibility is between 80 – 120 °C [3]. Van Gelder et al. [31] found that DSS (UNS
5 31803) when subjected to slow plastic strain was susceptible to SCC in sulphide - chloride
6 media at temperatures higher than 80 °C.
7
8
9
10
11
12
13

14 **3.2 Electrochemical corrosion – effects of ammonium bisulphite concentration**

15 The experimental set-up was based on the exposure of the SDSS mini pipe to 1000 ml of 0.1,
16 1 and 3.5 wt% NaCl solutions with the addition of various concentration of ammonium
17 bisulphite (0, 100, 500 and 1000 ppmw). Figure 8 shows the typical $\log(i)$ - E response for the
18 mini pipe specimens subject to no external loading in 0.1 and 3.5 wt% NaCl solution. The
19 forward scan was started just below the OCP or E_{corr} . Passivation was indicated by either
20 constant current or infinitesimal current increment over a finite potential range. This section
21 of the curve is referred to as the passive region. As the current and potential increase, a
22 breakdown in the passive film is inevitable unless the pipe is immune to corrosion in the
23 environment. When the potential increases to a point where growth of pits occur (metastable
24 pitting also visible), a breakdown potential (E_p) was determined. This potential was defined
25 as the point, which is beyond the passive region, where the current density suddenly
26 increases and exceeds 100 $\mu\text{A}/\text{cm}^2$.
27
28
29
30
31
32
33
34
35
36
37
38
39
40
41
42
43
44
45

46 The difference between OCP and E_p provides an indication of the resistance to pitting in all
47 the test environments. The OCP and E_p data from the polarisation curves are compared in
48 Table 4 for two nominally identical specimens. There was some slight variability in the
49 measured OCP and E_p , but test repeatability was generally good and most of the
50 corresponding data for the two nominally identical mini pipes are within 20 $\text{mV}_{\text{Ag}|\text{AgCl}}$ from
51
52
53
54
55
56
57
58
59
60

1
2
3 each other. The slight variation in the measured OCP and E_p for the two nominally identical
4 pipes may be due to clogged frit, decrease in saturation of the solution in the electrode or a
5 slight difference in pipe surface roughness. Overall the test results for the chloride-
6 ammonium bisulphite solution showed less variability in comparison to the chloride only
7 solution for OCP data because ammonium bisulphite works as a passivating inhibitor [10].
8
9
10
11
12
13

14
15
16
17 It was noted that the pitting potential, E_p , in the 3.5 wt% NaCl solution with the addition of
18 ammonium bisulphite was lower than the pitting potentials in the corresponding 0.1 and 1
19 wt% NaCl solutions apart from the 1 wt% NaCl plus 100 ppmw ammonium bisulphite.
20
21 Overall the trend of the $\log(i)$ - E plot (Figure 8) and pH measurement at ambient conditions
22 (Table 3) confirmed that 3.5 wt% NaCl solution (with or without the ammonium bisulphite)
23 had the most effect on pitting. This reinforces the assertion that the presence of chlorides is a
24 key component in the pitting of the external surface of the SDSS mini pipes at the test
25 temperature of 90 °C.
26
27
28
29
30
31
32
33
34
35
36
37

38 The addition of ammonium bisulphite generally resulted in the OCP becoming more negative
39 and in a reduction of the pitting resistance, determined by the pitting potential, E_p .
40 Ammonium bisulphite is a reducing agent and the reaction products in a chloride solution
41 include sulphide. As the concentration of the ammonium bisulphite increases the sulphide
42 level increases. The synergistic action of chloride and sulphide decreases the resistance to
43 pitting. This finding is consistent with the results obtained by Tsai et al. [32] who found the
44 corrosion potential of 2205 duplex stainless steel tensile samples shifted in the less noble
45 direction with increasing sulphide concentration in 3.5 wt% NaCl solutions.
46
47
48
49
50
51
52
53
54
55
56
57
58
59
60

1
2
3
4
5
6 Dissolved oxygen and pH can have a major effect on the corrosion behaviour of metals. In
7
8 the current study, the pH and DO were only measured at room temperature (see Table 3) and
9
10 not at the test temperature of 90 °C, as the test temperature was outside the working
11
12 temperature range of 50 °C for both the pH and DO meters. In an open system such as the
13
14 one considered in the current study, the DO decreases as the temperature is increased above
15
16 about 80 °C because oxygen is able to escape from the solution and the solubility of oxygen
17
18 decreases as the temperature is increased. The pH of the test solution is therefore expected
19
20 to decrease slightly as the temperature is increased from room temperature to 90 °C. It is
21
22 surmised that the effect of the small amount of DO and slight decrease in the pH due to the
23
24 elevated temperature on the corrosion behaviour of the material is negligible compared to
25
26 that of the solution, i.e. chloride-ammonium bisulphite.
27
28
29
30
31

3.3 Electrochemical corrosion – effects of external loading

32
33 The focus of the current study is the determination of the pitting potential in the various
34
35 chloride- ammonium bisulphite environments under combined loads, i.e. axial load and
36
37 internal pressure. Electrochemical polarisation studies of a pipe subject to combined loads in
38
39 an aqueous environment have seldom been reported. As the 3.5 wt% NaCl had the most
40
41 effect on pitting for the reference test, the potentiodynamic tests were carried out on the mini
42
43 pipe with load application in 3.5 wt% NaCl and various concentration of ammonium
44
45 bisulphite. An axial load of 568 MPa, internal pressure of 48.3 MPa, and combined axial
46
47 tension and internal pressure of 568 MPa and 48.3 MPa respectively were applied to the mini
48
49 pipe in all the solutions.
50
51
52
53
54
55
56
57
58
59
60

1
2
3
4
5
6
7
8
9
10
11
12
13
14
15
16
17
18
19
20
21
22
23
24
25
26
27
28
29
30
31
32
33
34
35
36
37
38
39
40
41
42
43
44
45
46
47
48
49
50
51
52
53
54
55
56
57
58
59
60

Polarisation curves are shown in Figure 9 for two nominally identical mini pipes subject to the combined axial tension and internal pressure in 3.5 wt% NaCl (Figure 9a) and in 3.5 wt% NaCl plus 100 ppmw of ammonium bisulphite (Figure 9b). There is a satisfactory level of consistency and repeatability in the results. The pitting potentials were 408 mV_{Ag|AgCl} (Pipe A), 390 mV_{Ag|AgCl} (Pipe B) in 3.5 wt% NaCl solution while the potentials were 520 mV_{Ag|AgCl} (Pipe A) and 503 mV (Pipe B) in 3.5 wt% NaCl plus 100 ppmw of ammonium bisulphite. Although most of the tests for each test condition were carried out on at least two nominally identical mini pipes, in the following only typical polarisation curves for one of the tested mini pipes for each test condition are presented due to the level of consistency in the results (as shown in Figure 9).

Figure 10 shows the polarisation curves for different loading conditions in the respective test solutions. The corrosion behaviour of the mini pipe in each solution was found to be stress and environment dependent. The polarisation curves for the mini pipes tested in each solution and load condition all exhibit anodic behaviour with distinct pitting potentials marked by a rapid rise in the current density.

The polarisation curves for $\log(i) - E$ response in 3.5 wt% NaCl (and no ammonium bisulphite) is compared in Figure 10a for different external loading conditions. The pitting potential shifted in the less noble direction with the application of external load and the potential range corresponding to the passive region decreased. The only exception was the axial tension test where the pitting potential was nobler than the reference test although there was indication of metastable pitting, initial pit growth (current density briefly exceeded 100

1
2
3 $\mu\text{A}/\text{cm}^2$), and temporary repassivation before continuous pit growth. The breakdown
4 potential for two nominally identical mini pipes subject to only axial tension was found to be
5
6 536 $\text{mV}_{\text{Ag}/\text{AgCl}}$ and 451 $\text{mV}_{\text{Ag}/\text{AgCl}}$. The pitting potentials for two mini pipes subject to internal
7
8 pressure only were found to be 363 $\text{mV}_{\text{Ag}/\text{AgCl}}$ and 324 $\text{mV}_{\text{Ag}/\text{AgCl}}$, which are slightly smaller
9
10 to the corresponding values for mini pipes subject to combined loading of 469 $\text{mV}_{\text{Ag}/\text{AgCl}}$ and
11
12 409 $\text{mV}_{\text{Ag}/\text{AgCl}}$.
13
14
15
16
17
18

19 The uniaxial strain at the onset of plastic yielding of the SDSS material under consideration
20
21 at the test temperature of 90 °C was found to be 0.3% [18]. The applied axial stress of 568
22
23 MPa was below the elastic limit, however for internal pressure only and combined loading,
24
25 the pipe was stressed beyond the elastic limit but below the level that caused burst or failure,
26
27 see Figure 6. The application of only axial tensile stress of 568 MPa, only internal pressure
28
29 of 48.3 MPa and a combined loading of axial stress of 568 MPa and internal pressure of 48.3
30
31 MPa induced respectively an axial strain of ϵ_a and a hoop strain ϵ_h of $(\epsilon_a, \epsilon_h) = (0.2\%, -$
32
33 $0.07\%), (0.1\%, 0.35\%)$ and $(0.55\%, 0.7\%)$ [27]. Thus, the pipes experienced some plastic
34
35 deformation when subject to only internal pressure of 48.3 MPa or combined loading axial
36
37 stress of 568 MPa and internal pressure of 48.3 MPa. It was observed that the pitting
38
39 potential E_p for specimens where the applied load resulted in plastic deformation (i.e.
40
41 internal pressure only and combined loading) is lower than that for specimens where there is
42
43 no plastic deformation (reference and axial tension only). A lower pitting potential observed
44
45 on the surface of the mini pipe under plastic deformation was due to the inherent instability
46
47 of the passive film during plastic deformation which would facilitate initiation sites for pits
48
49 in this environment. This is consistent with the findings of Renton et al. [33] which showed
50
51
52
53
54
55
56
57
58
59
60

1
2
3 that pitting potential of 25Cr SDSS subject to axial tension decreases with increasing level of
4 plastic deformation. It is important to note that a small change in wall thickness ($\pm 0.2 \mu\text{m}$
5 tolerance) can lead to a lower axial load capacity or higher strain in the pipe; thus, affect the
6 pitting potential. However, in addition to checks carried out to confirm pipe diameter the
7 consistency in the results of the mini pipe mechanical load tests to determine failure
8 envelope and the results of the corrosion tests particularly under various loads indicate that
9 the mini pipes were machined to the wall thickness specified, i.e. 0.25 mm. Although the
10 deformation of the mini pipe under various loading conditions would result in a nominal
11 increase in effective surface area; the same surface area was used to determine the pitting
12 potential for all mini pipes during the corrosion tests. For example, the mini pipe strain
13 during axial loading was 0.2% compared to 2.5% and a 4 mm elongation on failure; thus, the
14 increase in length of the mini pipe is negligible for the loading condition during the corrosion
15 tests. It should also be noted that for the axial loading tests there is slight reduction in the
16 diameter of the pipe due to compressive strain. For the internal pressure tests and combined
17 load tests the length of the pipe on failure was the same (60 mm); the hoop strain was 0.3%
18 on loading compared to above 2% on failure for the internal pressure tests [27]. Thus, the
19 change in effective surface area of the mini pipe during axial loading and pressure /
20 combined load tests was negligible due to material toughness demonstrated particularly in
21 the mechanical load tests [27]; thus, the use of the same surface areas would not alter the
22 conclusions of the electrochemical test results.
23
24
25
26
27
28
29
30
31
32
33
34
35
36
37
38
39
40
41
42
43
44
45
46
47
48
49
50

51 The general trend of the effect of loading on the polarisation curves for the specimens tested
52 in 3.5 wt% NaCl plus 100 ppmw ammonium bisulphite is similar to that for specimens tested
53
54
55
56
57
58
59
60

1
2
3 in 3.5 wt% NaCl without ammonium bisulphite (Figure 10a). However, the corrosion
4 potential for 3.5 wt% NaCl plus 100 ppmw ammonium bisulphite shifted more in the noble
5 direction with application of load and the potential range corresponding to the passive region
6 increased when compared with 3.5 wt% NaCl without ammonium bisulphite. The pitting
7 potentials for two nominally identical mini pipes subject to axial tension only in 3.5 wt%
8 NaCl plus 100 ppmw ammonium bisulphite were 511 mV_{Ag|AgCl} and 491 mV_{Ag|AgCl}; these are
9 not significantly different from the pitting potentials of 503 mV_{Ag|AgCl} and 520 mV_{Ag|AgCl} for
10 two identical specimens subject to combined load. Thus, the addition of 100 ppmw
11 ammonium bisulphite to the 3.5 wt% NaCl does not seem to have a detrimental effect on
12 pitting resistance.
13
14
15
16
17
18
19
20
21
22
23
24
25
26
27

28 The $\log(i)$ - E plot for the tests in 3.5 wt% NaCl plus 500 ppmw is shown in Figure 10b.
29 There was an indication of metastable pitting, initial pit growth (current density briefly
30 exceeded 100 $\mu\text{A}/\text{cm}^2$), and temporary repassivation before continuous pit growth when the
31 SDSS pipes were subjected to load in both solutions. Unlike the 3.5 wt% NaCl plus 100
32 ppmw ammonium bisulphite, when external load is applied to the SDSS mini pipes in 3.5
33 wt% NaCl plus 500 ppmw and 1000 ppmw ammonium bisulphite, the interaction between
34 ion dissolution and the passive film in addition to the formation of sulphide (protective) at pit
35 initiation sites lead to a decrease in pitting resistance due to increased ammonium bisulphite
36 concentration and a synergistic effect with chloride which reduces the pH. An overview of
37 the interaction between test environment and the iron that forms a significant part of the
38 SDSS composition (Table 1) is provided in equation 2.
39
40
41
42
43
44
45
46
47
48
49
50
51
52
53
54
55
56
57
58
59
60



The pitting potentials in 3.5 wt% NaCl plus 500 ppmw ammonium bisulphite were 308 mV_{Ag|AgCl} and 304 mV_{Ag|AgCl} for two nominally identical mini pipes subject to combined load, and 385 mV_{Ag|AgCl} and 363 mV_{Ag|AgCl} for two mini pipes subject to combined load in 3.5 wt% NaCl plus 1000 ppmw ammonium bisulphite. Similarly the pitting potential for the mini pipe subject to axial tension in 3.5 wt% NaCl plus 500 ppmw and 1000 ppmw ammonium bisulphite respectively were 380 mV_{Ag|AgCl}, 321 mV_{Ag|AgCl} and 359 mV_{Ag|AgCl}, 316 mV_{Ag|AgCl}; for internal pressure only it was 376 mV_{Ag|AgCl}, 406 mV_{Ag|AgCl} and 372 mV_{Ag|AgCl}, 332 mV_{Ag|AgCl} respectively. Thus, the increase in the concentration of ammonium bisulphite to 500 ppmw and 1000 ppmw had a similar detrimental effect on pitting resistance.

The effect of ammonium bisulphite and external load on the average pitting potential is shown in Figure 11. The average pitting potential for the mini pipes subject to only axial tension was not significantly different from that subject to combined load for all the various concentration of ammonium bisulphite considered (see Figure 11). The load in the axial tension test was within the elastic limit but when internal pressure was additionally applied the pipe was stressed beyond elastic limit but below the axial tension – internal pressure combination required for failure [27]; thus, the pipe with induced plastic deformation was more susceptible to pitting.

The pH of the 3.5 wt% NaCl solution without ammonium bisulphite measured at 25 °C was 7 while the pH was between 4.5 and 5.5 with the addition of varying concentration of

1
2
3 ammonium bisulphite (see Table 3). It was not possible to measure the pH of the bulk
4 solution in situ at the test temperature (90 °C) due to electrode temperature limit (50 °C).
5
6 Although, the pH of the bulk solution will decrease slightly with increase in temperature
7
8 from ambient to 90 °C, there is evidence to suggest that E_p of stainless steel is independent
9
10 of pH below 8.5 of the bulk solution [34]. Turnbull and Ferriss found a decrease in pH in
11
12 cracks in 3.5 wt% NaCl compared to the pH of the bulk solution [31]. Although there is no
13
14 measured data of pH inside the pits from the current series of tests, based on published
15
16 results for low alloy steel [35], the pH inside the pits for the SDSS pipes is expected to be
17
18 lower than the pH of the bulk solution which sustains further corrosion activity and pit
19
20 growth.
21
22
23
24
25
26
27
28

29 In the reference test (no stress applied), the pipe relies mainly on the passive film for
30 protection from corrosion. However, when load is applied there will be some dissolution of
31 iron (Fe), chromium (Cr) etc. According to Pourbaix [36], all sulphur substances with
32 oxidation numbers between the extreme -2 (sulphides) and +6 (sulphates), except for solid
33 sulphur (oxidation number 0), are thermodynamically unstable and tend to decompose; thus
34 sulphite (oxidation number +4) is unstable in water. In addition, ammonium bisulphite is a
35 reducing agent and functions mainly as passivating corrosion inhibitor in addition to
36 scavenging of oxygen [10]. Hemmingsen et al. [37] found that sulphide films are formed on
37 carbon steel in sulphite solutions. Thus, it appears that in the tests where external load is
38 applied the interaction between ion (primarily Fe and Cr) dissolution (due to the stress
39 stabilisation process) and the passive film, in addition to the formation of sulphide protective
40 film, at pit initiation sites initially leads to an increase in pitting resistance at low ammonium
41
42
43
44
45
46
47
48
49
50
51
52
53
54
55
56
57
58
59
60

1
2
3 bisulphite concentration. However, as the concentration increases beyond 100 ppmw the
4
5 presence and increase in sulphide leads to a decrease in pitting resistance.
6
7

8
9
10 Ammonium bisulphite enhances the cathodic reaction which is consequently balanced by the
11
12 anodic reaction, since the increase in ammonium bisulphite concentration in the 3.5 wt%
13
14 NaCl solution causes E_{corr} of the SDSS mini pipe to shift to a more negative potential. This
15
16 implies that the ammonium bisulphite polarises the cathodic reaction and thus acts as a
17
18 cathodic inhibitor for the pipe thereby decreasing the rate of hydrogen evolution and SCC of
19
20 the SDSS pipes. However, at pit initiation sites the activity of the anodic reaction will
21
22 produce hydrogen that gets absorbed in SDSS pipe as the presence of sulphide inhibits the
23
24 recombination of atomic hydrogen (H^+). The atomic hydrogen recombines within the SDSS
25
26 pipe microstructure to molecular hydrogen (H_2) leading to crack initiation.
27
28
29

30
31
32
33 Hydrogen ion concentration is a measure of pH; the higher the hydrogen ion concentration,
34
35 the lower the pH. As the pH decreases, corrosion activity increases [16]. Thus, as the
36
37 sulphite concentration in the solution (3.5 wt% NaCl) increases the pH of the solution
38
39 slightly decreases (Table 3). The resistance of the SDSS pipes to pitting increased with the
40
41 addition of 100 ppmw ammonium bisulphite to 3.5 wt% NaCl but decreased with further
42
43 additions of ammonium bisulphite (500 and 1000 ppmw) when subject to various load
44
45 conditions (axial tension, internal pressure and combined loading), see Figure 11. This
46
47 suggests that the diffusion and migration processes of bisulphite / chloride ions have more of
48
49 an effect on passive film growth and pit chemistry of the SDSS pipes in this environment
50
51 when subjected to stress. The change in the surface stress is a key factor in the initiation of
52
53
54
55
56
57
58
59
60

1
2
3 pits [38]. Fatah et al. [39] found that the sulphide ions are easily adsorbed on mild steel
4 surface, by occupying active sites on the steel surface, thereby accelerating the rate of steel
5 dissolution. Thus, the optimum concentration for maximum resistance of the SDSS pipe
6 under the various load conditions as illustrated in Figure 11 is 100 ppmw ammonium
7 bisulphite.
8
9
10
11
12
13
14
15
16

17 In comparison to the reference (no external load), the pitting resistance was affected more by
18 internal pressure than combined load in 3.5 wt% NaCl and 3.5 wt% NaCl plus 100 ppmw
19 ammonium bisulphite solution, while there was negligible effect of external loading on the
20 pitting corrosion behaviour of the SDSS pipes in 3.5 wt% NaCl plus 500 ppmw and 1000
21 ppmw ammonium bisulphite. It seemed the ammonium bisulphite concentration was high
22 enough to provide a protective film on the surface of the pipe thereby produce similar
23 resistance quantitatively.
24
25
26
27
28
29
30
31
32
33
34

35 **3.4 Scanning electron microscope (SEM) observation**

36 Careful SEM examination of the surface of the pipe after anodic polarisation confirmed that
37 the increase in current density was due to initiation of pits. Individual pits and sometimes
38 cluster of pits and cracks were observed. Pits were observed on all the mini pipes exposed to
39 the different solutions with or without external load. The pit morphology on the external
40 surface of SDSS pipes were similar in all the environment considered however the pits tend
41 to be less frequent with the addition of ammonium bisulphite to the sodium chloride solution
42 (Figure 12). This observation implies that the ammonium bisulphite works as a passivating
43 inhibitor which reduces the number of pit initiation sites.
44
45
46
47
48
49
50
51
52
53
54
55
56
57
58
59
60

1
2
3 In the anodic potentiodynamic tests, the current output provided information on the growing
4 pits as the applied potential increased. As ammonium bisulphite concentration increased the
5 number of pits initiated was less; thus, the cathodic current increased and was balanced by
6 the increase in anodic current resulting in increased pit growth (associated with hydrogen
7 evolution within the pit and further acidification) at discrete points. The hydrogen produced
8 by the electrochemical reaction may readily diffuse into the metal structure with consequent
9 detrimental effect on the mechanical strength and ductility of the metal.
10
11
12
13
14
15
16
17
18
19
20

21 The pits on the external surface of the SDSS pipes in sodium chloride solution (without
22 ammonium bisulphite) contained little or no deposits while the pits on the pipes tested in
23 sodium chloride plus various concentration of ammonium bisulphite usually contained
24 corrosion deposits. The amount of deposits appeared to increase with increasing ammonium
25 bisulphite concentration (Figure 13). The presence of deposits will facilitate pit growth. Ernst
26 and Newman [40] found precipitation of metal salt takes place (at the pit bottom) and the pit
27 grows underneath the salt film at a rate controlled by the dissolution of this film and local
28 concentration gradient. It is expected that the addition of ammonium bisulphite to the sodium
29 chloride solution will have more of an effect on the concentration gradient of the bulk
30 solution and pit interior compared to sodium chloride solution due to the type of deposits in
31 the pits.
32
33
34
35
36
37
38
39
40
41
42
43
44
45
46
47
48

49 Visual examination of the deposit suggests the pits on the pipes tested in 3.5wt% NaCl
50 solution contained sodium chloride salt deposit while the pits on pipes tested in sodium
51
52
53
54
55
56
57
58
59
60

chloride / ammonium bisulphite contained a mixture of sodium chloride and ammonium salts.

Although pits were identified on the surface of most of the samples tested under external load, only SDSS pipes subject to internal pressure or combined load showed any signs of crack initiation from the pits which formed during the electrochemical tests (Figure 14). The polishing marks that are visible in Figure 14 are parallel to the hoop direction, and cracks which initiated from the pits appear to grow perpendicular to the hoop direction. The surface finish of the mini pipe was higher than the surface finish required for test samples in standards for four-point bend, C ring and tensile samples i.e. 0.7 [41], 0.7 [42] and 0.25 μm [43] respectively. The wall thickness was machined to within 0.2 μm tolerance to ensure that the wall thickness of the mini pipes (0.25 mm) were consistent as confirmed by the failure loads test results compared to theory (Figure 6). Thus, a higher surface finish (compared to standard test samples) was accepted for the mechanical and corrosion tests. The surface finish did not affect the mechanical [27] or corrosion tests as test results were consistent as illustrated in the failure envelope test and polarisation results (Figure 9). Furthermore, the surface finish did not affect the crack initiation and orientation. Rajaguru and Arunachalam in their investigation on machining induced surface and subsurface modifications on the SCC growth behavior of SDSS found clusters, parallel and perpendicular cracks [44]. Only perpendicular cracks were found during SEM investigation of the mini pipes. The pipe was closed at one end (Figure 3) and pressurised through the other (Figure 5). Three load cases were considered: axial tensile stress of 568 MPa ($= 0.64\sigma_{0.2}$); internal pressure of 48.3 MPa, which induced a hoop stress of 773 MPa in the pipe; and a combined axial stress of 568 MPa and hoop stress of 773 MPa. The major principal stress for internal pressure and combined

1
2
3 loading conditions was the hoop stress. Based on maximum principal stress failure criterion,
4 crack initiation and growth occur perpendicular to the maximum principal stress. The
5
6 observed direction of crack growth is consistent with the maximum principal stress criterion.
7
8
9
10 The internal pressure applied in the current tests was based on 0.85 times the measured burst
11
12 pressure at 90 °C. This indicates that the SDSS pipes under internal pressure or combined
13
14 axial tension and internal pressure are susceptible to SCC in the various test environments.
15
16 Thus, the internal pressure of 48.3 MPa in the mini SDSS pipes considered in this study
17
18 exceeded the threshold for initiation of SCC in the test environment. Cracks will initiate and
19
20 grow from a pit as pits introduce local stress concentration which promotes crack growth and
21
22 affects the effectiveness of the passive film and inhibitor (ammonium bisulphite) films as a
23
24 barrier to mitigate further corrosion.
25
26
27
28
29

30
31 The mini pipes subject to axial tension and those with no external load (i.e. reference
32
33 specimen) exhibited only pitting in all test environments as confirmed by the SEM images.
34
35 The stresses in both tests were within the elastic limit of the SDSS pipes and yield stress at
36
37 room temperature and test temperature are similar (Table 2); thus, as expected, the
38
39 environment effect was more significant, as the corrosivity (decrease in pH) increases
40
41 (illustrated by potentiodynamic tests). In the group of mini pipes which were under
42
43 combined loading the stress level was always beyond the elastic limit of the material. In such
44
45 circumstance not only were pits observed there was also initiation of cracks. This confirms a
46
47 stress effect and susceptibility to cracking in all test environments for pipes subject to
48
49 combined loading. In the test environments considered in this study it is expected that crack
50
51 initiation could be prevented by lowering the applied internal pressure to 40 MPa; this is the
52
53
54
55
56
57
58
59
60

1
2
3 pressure when the pressure versus hoop strain response changes from being linear to
4 nonlinear [27]. The threshold load for SCC initiation in the SDSS pipe under internal
5
6
7
8 pressure and combined load requires further investigation.
9

10 11 12 **4 CONCLUSIONS**

13 The corrosion behaviour of 25Cr SDSS mini pipe subject to axial tension, internal pressure,
14 and combined load (axial tension and internal pressure) was investigated in 3.5 wt% NaCl
15
16
17 solution with various concentration of ammonium bisulphite (0, 100, 500 and 1000 ppmw)
18
19
20 and at a temperature of 90 °C. The external surface of the mini pipe was exposed to the test
21
22
23 environment, the corrosion potential versus current density measurements was determined.
24
25 From the experimental results obtained from this study, the following conclusions can be
26
27
28 made:
29
30
31

- 32 1. Pitting was observed under all exposure conditions on the external surface of the
33
34 pipe. However, the addition of ammonium bisulphite was found to reduce the density
35
36 of pits and to increase the severity of the remaining pits left on the surface of the
37
38 pipe. The presence of chlorides is a key component in the pitting of the external
39
40 surface of the SDSS mini pipes at 90 °C. The increase in chloride from 0.1 to 1 and to
41
42 3.5 wt% and the addition of ammonium bisulphite generally resulted in increased
43
44 active values for the corrosion potential and decreased the pitting resistance. The
45
46 resistance of the SDSS pipes to pitting when subject to various load conditions
47
48 (combined axial tension and internal pressure, axial tension and internal pressure)
49
50 increased slightly with the addition of 100 ppmw ammonium bisulphite to 3.5 wt%
51
52 NaCl but decreased with further additions of ammonium bisulphite (500 and 1000
53
54
55
56
57
58
59
60

1
2
3 ppmw). Thus, the optimum concentration for maximum resistance of the SDSS pipe
4
5 to pitting corrosion under the various load conditions is 100 ppmw ammonium
6
7 bisulphite in 3.5 wt% NaCl.
8
9

- 10
11
12 2. The pitting resistance of the SDSS pipe was found to be affected more by internal
13
14 pressure than combined load in 3.5 wt% NaCl and 3.5 wt% NaCl plus 100 ppmw
15
16 ammonium bisulphite solution. The pitting potentials of the mini pipes subjected to
17
18 axial tension, combined axial tension and internal pressure in 3.5 wt% NaCl plus 500
19
20 ppmw and 1000 ppmw ammonium bisulphite were quite similar; the pitting
21
22 resistance of the SDSS pipe in both solutions under the same loading condition were
23
24 less than in the 3.5 wt% NaCl and 3.5 wt% NaCl plus 100 ppmw ammonium
25
26 bisulphite solution.
27
28
29
30
31
32
33 3. Crack initiation from pits was observed in specimens subjected to internal pressure
34
35 and combined internal pressure and axial tension, while none was observed in
36
37 specimens, subject to only axial tension. The internal pressure applied was 0.85 and
38
39 0.72 of the burst pressure at 90 °C and room temperature respectively. Therefore, the
40
41 internal pressure of 48.3 MPa exceeds the threshold for initiation of SCC in the test
42
43 environment considered in this study.
44
45
46
47
48

49 Material selection for production tubings used in oil and gas well completions is based on
50
51 qualification (corrosion) tests in relevant environments usually from test samples subject to
52
53 simple mode loading. Material selection for production tubing used in well completions
54
55
56
57
58
59
60

1
2
3 requires an understanding of the relationship between service stresses caused by load (weight
4 of tubing string) and pressure and the ability of the material to resist crack initiation in
5 service. Therefore, rather than conventional test samples, the use of mini pipes is proposed to
6 better define application limits in corrosive environments either by potentiodynamic tests
7 and/or immersion tests once the failure envelope is determined in the absence of any
8 corrosive environment.
9
10
11
12
13
14
15
16
17
18

19 **ACKNOWLEDGEMENTS**

20
21 The financial support of Shell UK is acknowledged. The authors would like to thank the
22 following technical staff, Stuart Herbert, Alistair Robertson for the machining of the mini
23 pipes, Derek Logan and Irene Brand for resolving several electrical issues and providing
24 accessories, and Jim Gall for help with the test set-up and prompt supply of tools and
25 equipment.
26
27
28
29
30
31
32
33
34
35
36
37
38
39
40
41
42
43
44
45
46
47
48
49
50
51
52
53
54
55
56
57
58
59
60

REFERENCES

- [1] A. Turnbull, S. Zhou, *Corr. Sci.* **2004**, 46, 1239.
- [2] A. Turnbull, L. N. McCartney, S. Zhou, *Corr. Sci.* **2006**, 48, 2084.
- [3] J. Oredsson, S. Bernhardsson, *Material Performance*, **1983**, 1, 34.
- [4] H. Tsuge, *The Sumitomo Search*, **1988**, 5, 65.
- [5] L. Cao, A. Anderko, F. Gui, N. Sridhar, *Corrosion*, **2016**, 72, 636.
- [6] E. Mazario, R. Venegas, P. Herrasti, M.C. Alonso, F.J. Recio, *Journal of Solid State Electrochemistry*, **2016**, 20, 1223.
- [7] D. E. Mowat, M.C. Edgerton, E. H. R. Wade, presented at *SPE/IADC Drilling Conference*, Amsterdam, Netherlands, 27 February - 1 March, **2001**, Paper No. 67779.
- [8] R. Mack, C. Williams, S. Lester, J. Casassa, presented at *Corrosion 2002*, Denver, Colorado, USA, 7 - 11 April, **2002**, Paper No. 2067.
- [9] I. M. Hannah, D. A. Seymour, presented at *Corrosion 2006*, San Diego, California, USA, 12 - 16 March, **2006**, Paper No. 06491.
- [10] NACE International Task Group T-3A-6, *Oxygen Scavengers in Steam Generating Systems and in Oil Production*, NACE Item No. 24177, **1994**.
- [11] B. A. Lasebikan, A. R. Akisanya, W. F. Deans, D. E. Macphee, *Corr. Sci.* **2011**, 53, 4014.
- [12] N. Zhou, R. Pettersson, R. Lin Peng, M. Schonning, *Materials Science and Engineering*, **2016**, 658, 50.

- 1
2
3 [13] H. P. Seifert, R. Ritter, *Corr. Sci.* **2016**, 108, 134.
4
5
6 [14] L. Wickstrom, K. Mingard, G. Hinds, A. Turnbull, *Corr. Sci.* **2016**, 109, 86.
7
8
9 [15] J. Soltis, *Corr. Sci.* **2015**, 90, 2.
10
11
12 [16] A. Keitelman and M. G. Alvarez, *Corrosion*, **2017**, 73, 8.
13
14 [17] E Hornlund, J.K.T. Fossen, S, Hauger, C. Haugen, T. Havn, T. Hemmingsen, *Int. J. of*
15
16 *Electrochem. Sci.*, **2007**, 2, 82.
17
18
19 [18] B. A. Lasebikan, A. R. Akisanya, W. F. Deans, *J. Materials Engineering and*
20
21 *Performance*, **2013**, 22, 598.
22
23
24 [19] H. Hanninen, J. Romu, R. Ilola, J. Tervo, and A. Laitinen, *J. Mater. Proc. Tech.*, **2001**,
25
26 117, 424.
27
28
29 [20] J. Airao, B. Chaudhary, V. Bajpai, N. Khanna, *Materials Today: Proceedings*, **2018**, 5,
30
31 3682.
32
33
34 [21] ASTM G48-03, *Standard Test Methods for Pitting and Crevice Corrosion Resistance*
35
36 *of Stainless Steels and Related Alloys by Use of Ferric Chloride Solution*, **2003**.
37
38
39 [22] X. Xu, M. Zhao, Y. Feng, F. Li, X. Zhang, *Int. J. Electrochem. Sci.*, **2018**, 13, 4298.
40
41
42 [23] G. Chail, P. Kangas, *Procedia Structural Integrity*, **2016**, 2, 1755.
43
44
45 [24] ASTM G5-94 (Reapproved 2004), *Standard reference test method for making*
46
47 *potentiostatic and potentiodynamic anodic polarisation measurements*, **2004**.
48
49
50 [25] B. A. Lasebikan, A. R. Akisanya, W. F. Deans, *J. Eng. Design and Technology*, **2015**,
51
52 13, 539.
53
54
55
56
57
58
59
60

- 1
2
3 [26] ASTM G150-99 (Reapproved 2004), *Standard Test Method for Electrochemical*
4 *Critical Pitting Temperature Testing of Stainless Steel*, **2004**.
5
6
7
8 [27] B.A. Lasebikan, A.R. Akisanya, *Int. J. Pres. Vessel and Piping*, **2014**, 119, 62.
9
10
11 [28] U. Obi, *Ph. D. Thesis*, University of Aberdeen, **2015**.
12
13
14 [29] L. He, Y.-J. Guo, X. -Y, Wu, Y. -M. Jiang, J. Li, *J. of Iron and Steel Research*
15 *International*, **2016**, 23, 357.
16
17
18 [30] G. Hinds, L. Wickstrom, K. Mingard, A. Turnbull, *Corr. Sci.* **2013**, 71, 43.
19
20
21 [31] K. van Gelder, J. G. Erlings, J. W. M. Damen, A. Visser, *Corr. Sci.* **1987**, 27, 1271.
22
23
24 [32] S. T. Tsai, K. P. Yen, H. C. Shih, *Corr. Sci.* **1998**, 40, 281.
25
26
27 [33] N.C. Renton, A.M. Elhoud, W.F. Deans, *J. of Mater. Engineering and Performance*,
28 **2011**, 20, 436.
29
30
31 [34] B. Tzaneva, *J. Chem. Tech. Metall.* **2013**, 48, 383-390.
32
33
34 [35] A. Turnbull, D. H. Ferriss, *Corr. Sci.* **1987**, 27, 1323.
35
36
37 [36] M. Pourbaix, *Atlas of electrochemical equilibria in aqueous solutions*, Pergamon Press
38 Ltd. Great Britain, **1966**.
39
40
41 [37] T. Hemmingsen, F. Fusek, E. Skavås, *Electrochimica Acta*, **2006**, 51, 2919.
42
43
44 [38] V. Vignal, O. Delrue, O. Heintz, J. Peultier, *Electrochimica Acta*, **2010**, 55, 7118.
45
46
47 [39] M. C. Fatah, M. C. Ismail, B. Ari-Wahjoedi, K. A. Kurnia, *Material Chemistry and*
48 *Physics*, **2011**, 127, 347.
49
50
51 [40] P. Ernst, R. C. Newman, *Corr. Sci.* **2002**, 44, 927.
52
53
54
55
56
57
58
59
60

- 1
2
3 [41] ASTM G39-99, (Reapproved 2005). *Standard practice for preparation and use of bent*
4 *beam, stress-corrosion test specimens, 2005.*
5
6
7
8 [42] ASTM G38-01, *Standard practice for making and using C-ring stress-corrosion test*
9 *specimens, 2001.*
10
11
12
13 [43] ASTM G129-00, *Standard practice for slow strain rate testing to evaluate the*
14 *susceptibility of metallic materials to environmentally assisted cracking, 2000.*
15
16
17
18 [44] J. Rajaguru, N. Arunachalam, *Corr. Sci.* **2018**, 141, 230.
19
20
21
22
23
24
25
26
27
28
29
30
31
32
33
34
35
36
37
38
39
40
41
42
43
44
45
46
47
48
49
50
51
52
53
54
55
56
57
58
59
60

Table 1- Pipe Chemical Composition percent by weight.

Elements	wt%
Carbon	0.02
Silicon	0.036
Manganese	0.049
Phosphorus	0.026
Sulphur	<0.015
Chromium	24.5
Molybdenum	3.27
Nickel	6.83
Copper	0.49
Vanadium	0.09
Cobalt	0.11
Titanium	2.61
Nitrogen	0.32
Iron	Balance

Table 2 - The average uniaxial tensile properties of the 25Cr SDSS at room temperature (18 °C) and elevated temperature of 90 °C

Temperature (°C)	18	90
Yield Stress (MPa)	601	601
0.2% Proof Stress (MPa)	969	881
Tensile Strength (MPa)	1063	948
Young's Modulus (GPa)	208	207

Table 3 - The pH and dissolved oxygen of the test solution containing different ammonium bisulphite concentration.

(a) pH

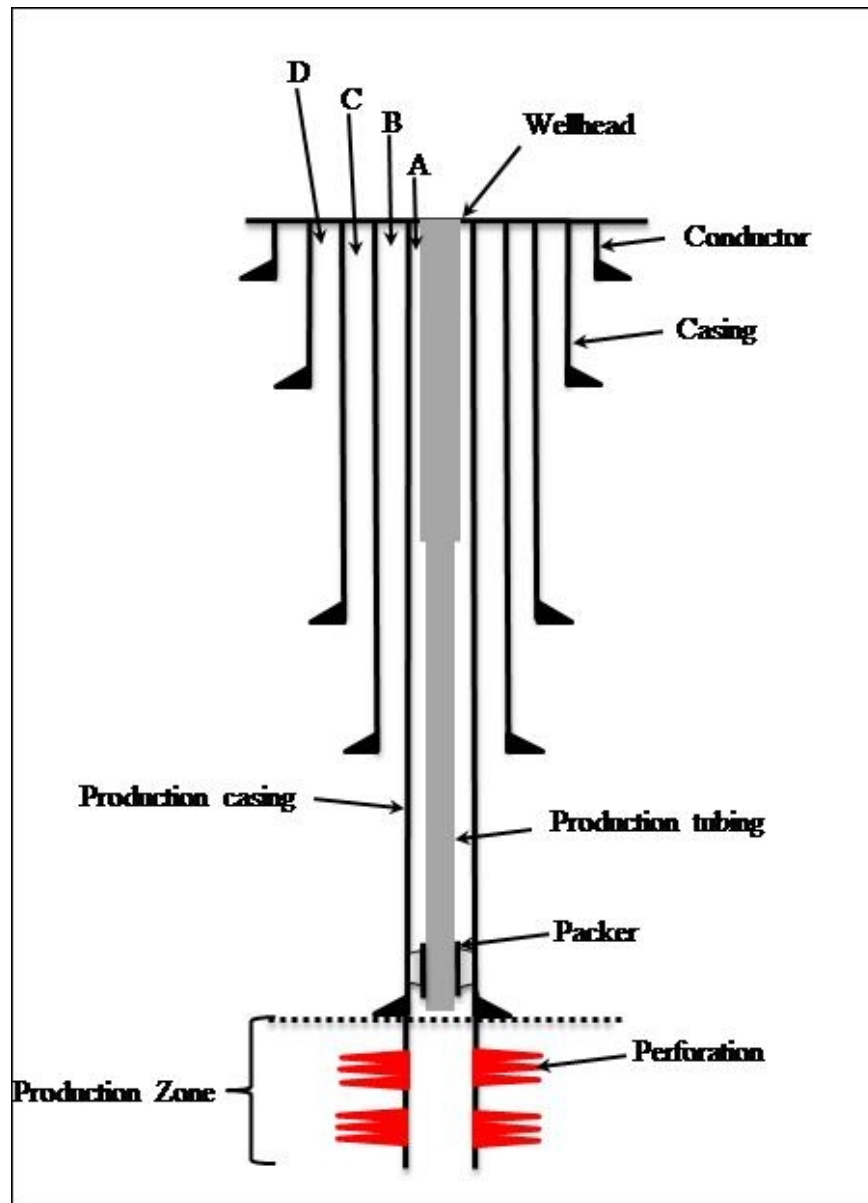
Solution	Ammonium bisulphite concentration (ppmw)			
	0	100	500	1000
Deionised Water	6.9	5.5	5.3	5.2
1 wt% NaCl	6.8	5.2	4.9	4.9
3.5 wt% NaCl	7.3	4.8	4.7	4.5

(b) Dissolved oxygen (ppbw)

Solution	Ammonium bisulphite concentration (ppmw)			
	0	100	500	1000
Deionised Water	4100	5740	5720	5990
1 wt% NaCl	5390	5750	5830	5150
3.5 wt% NaCl	4870	4440	4510	4100

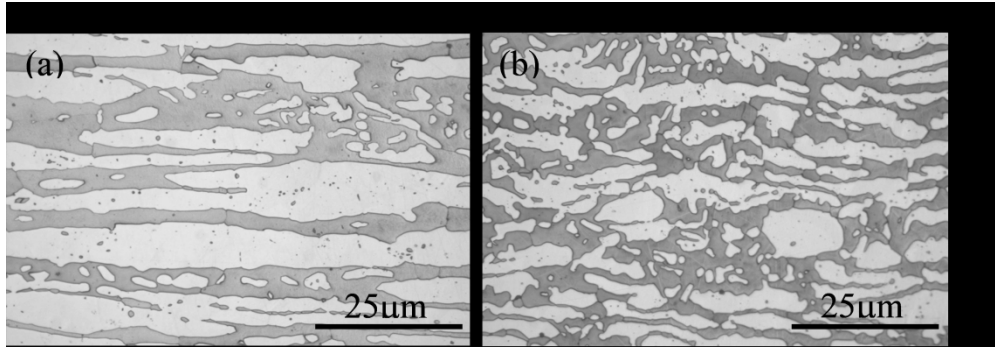
Table 4 - OCP and E_p of the mini pipe in various test solutions (sodium chloride and ammonium bisulphite) with no loads applied. Results are shown for two nominally identical mini pipes, identified as A and B. The values are in Volts relative to Ag|AgCl reference electrode.

Solution	A		B	
	OCP	E_p	OCP	E_p
0.1 wt% NaCl	-0.148	0.469	-0.156	0.586
0.1 wt% NaCl + 100 ppmw	-0.186	0.714	-0.185	0.757
0.1 wt% NaCl + 500 ppmw	-0.184	0.723	-0.182	0.705
0.1 wt% NaCl + 1000 ppmw	-0.203	0.693	-0.203	0.695
1 wt% NaCl	-0.161	0.480	-0.178	0.520
1 wt% NaCl + 100 ppmw	-0.379	0.259	-0.386	0.289
1 wt% NaCl + 500 ppmw	-0.402	0.402	-0.404	0.570
1 wt% NaCl + 1000 ppmw	-0.386	0.426	-0.390	0.429
3.5 wt% NaCl	-0.152	0.458	-0.160	0.484
3.5 wt% NaCl + 100 ppmw	-0.284	0.369	-0.289	0.343
3.5 wt% NaCl + 500 ppmw	-0.298	0.332	-0.292	0.349
3.5 wt% NaCl + 1000 ppmw	-0.304	0.423	-0.312	0.405



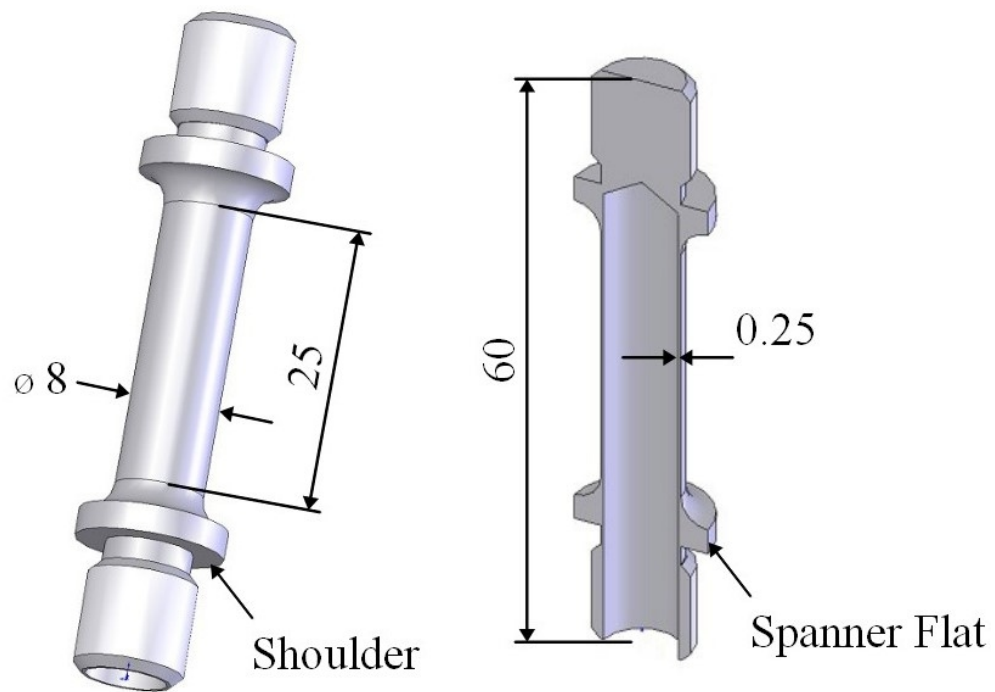
A schematic of a typical well completion system

119x164mm (96 x 96 DPI)



Microstructure of SDSS (a) longitudinal and (b) transverse direction

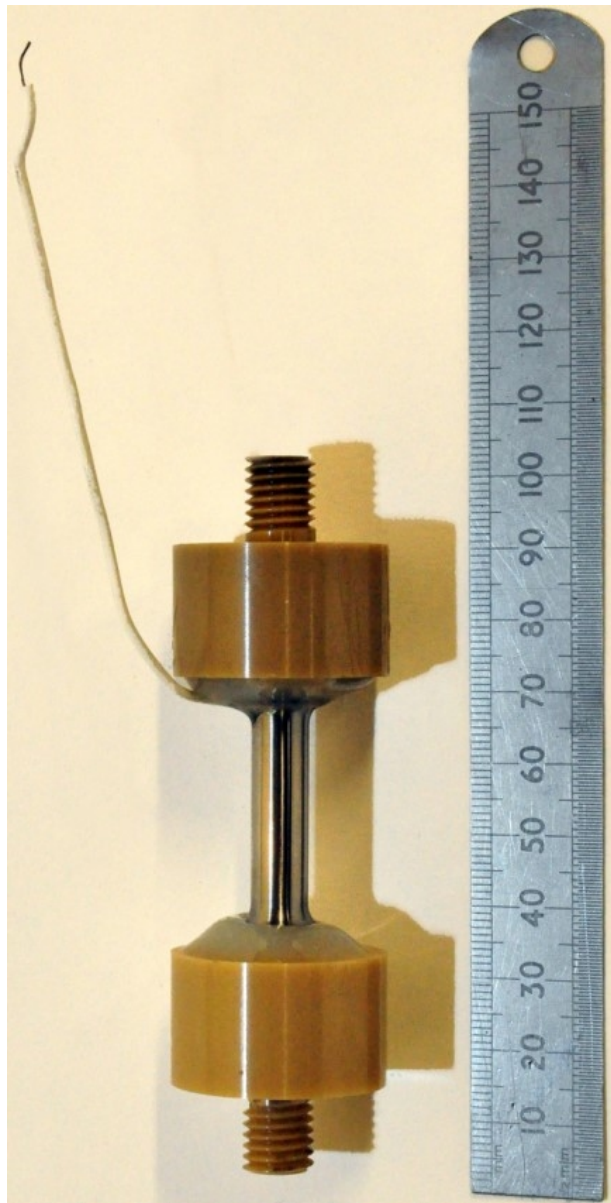
997x343mm (96 x 96 DPI)



The mini pipe (all dimensions in mm)

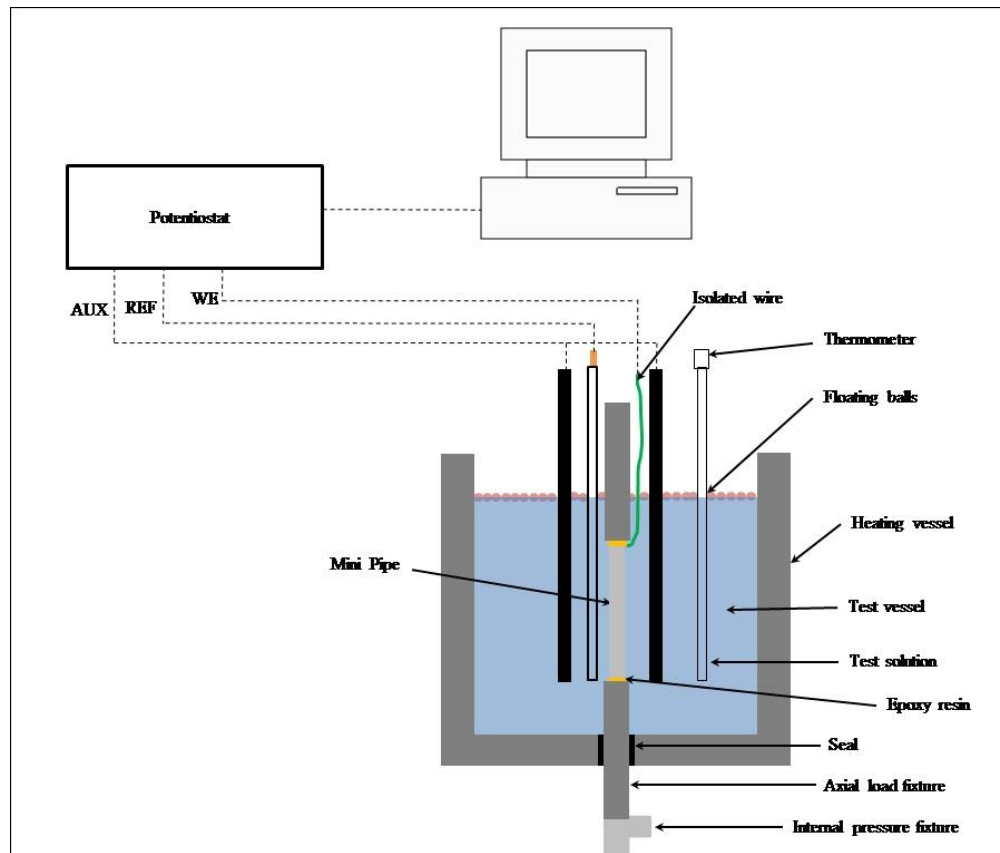
217x150mm (96 x 96 DPI)

1
2
3
4
5
6
7
8
9
10
11
12
13
14
15
16
17
18
19
20
21
22
23
24
25
26
27
28
29
30
31
32
33
34
35
36
37
38
39
40
41
42
43
44
45
46
47
48
49
50
51
52
53
54
55
56
57
58
59
60



Mini pipe set-up for corrosion test

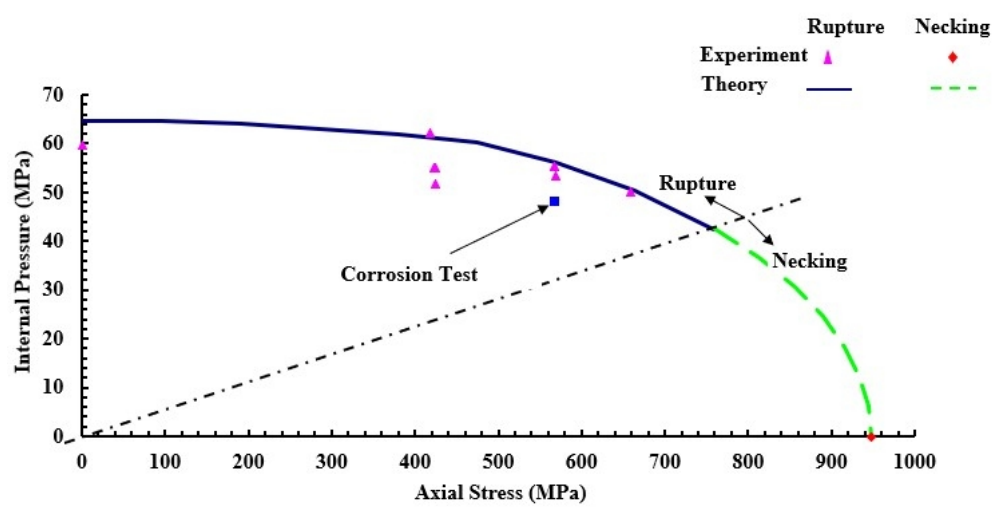
50x98mm (220 x 220 DPI)



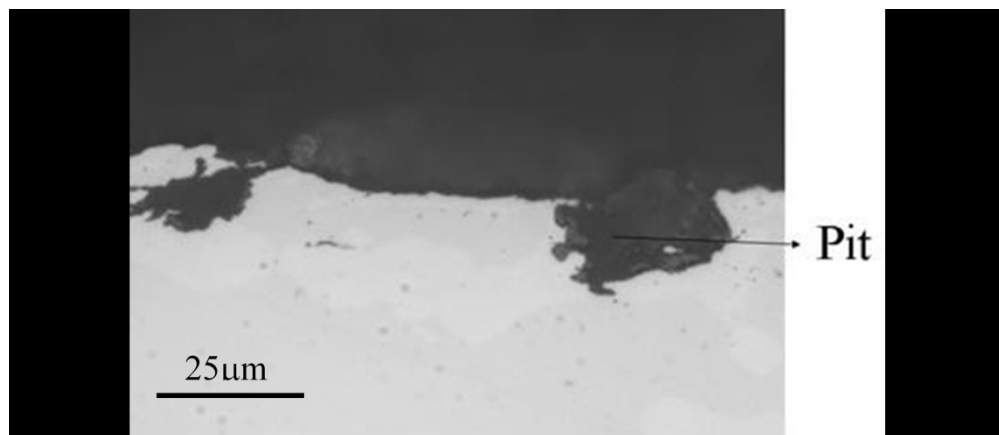
A schematic of the electrochemical polarisation test set-up

237x201mm (96 x 96 DPI)

1
2
3
4
5
6
7
8
9
10
11
12
13
14
15
16
17
18
19
20
21
22
23
24
25
26
27
28
29
30
31
32
33
34
35
36
37
38
39
40
41
42
43
44
45
46
47
48
49
50
51
52
53
54
55
56
57
58
59
60

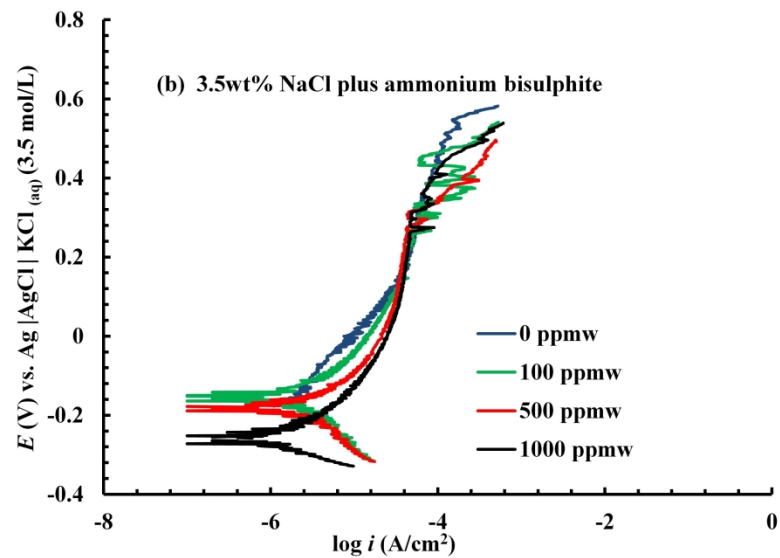
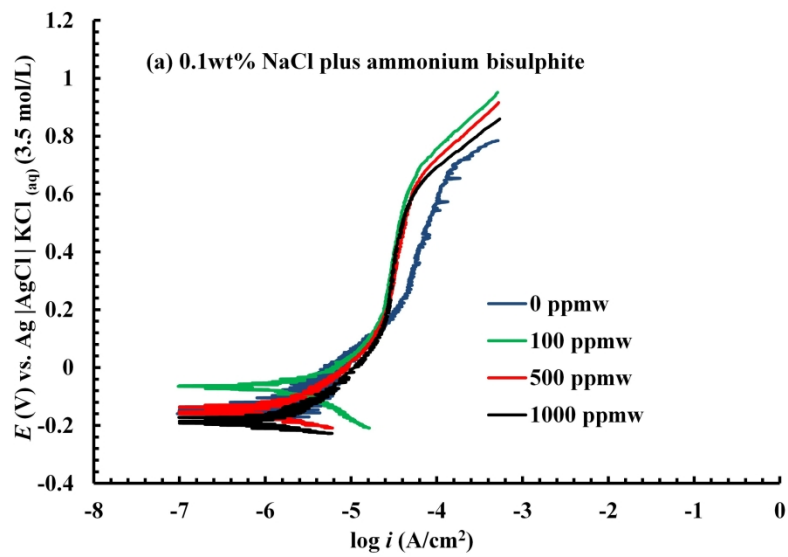


Corrosion test data point in mini pipe failure envelope at 90 oC
197x105mm (96 x 96 DPI)



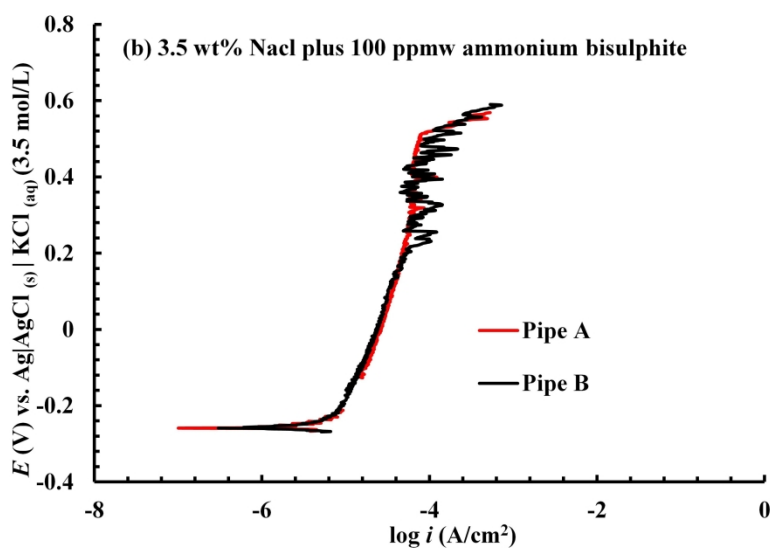
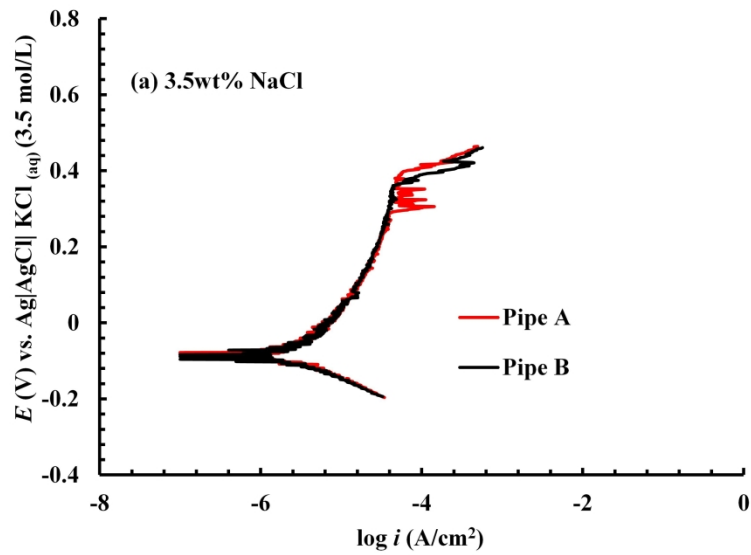
Micrograph of the cross-section of a pit after immersion test

997x429mm (96 x 96 DPI)



45 Polarisation scan of mini pipes for the reference tests where the mini pipes were not subjected to external
46 load in (a) 0.1wt% NaCl solution and (b) 3.5 wt% NaCl solution

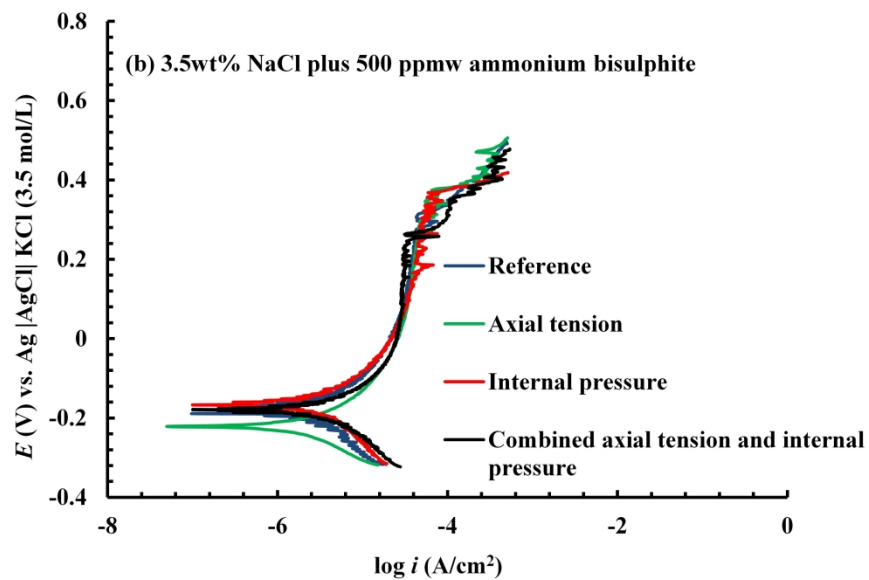
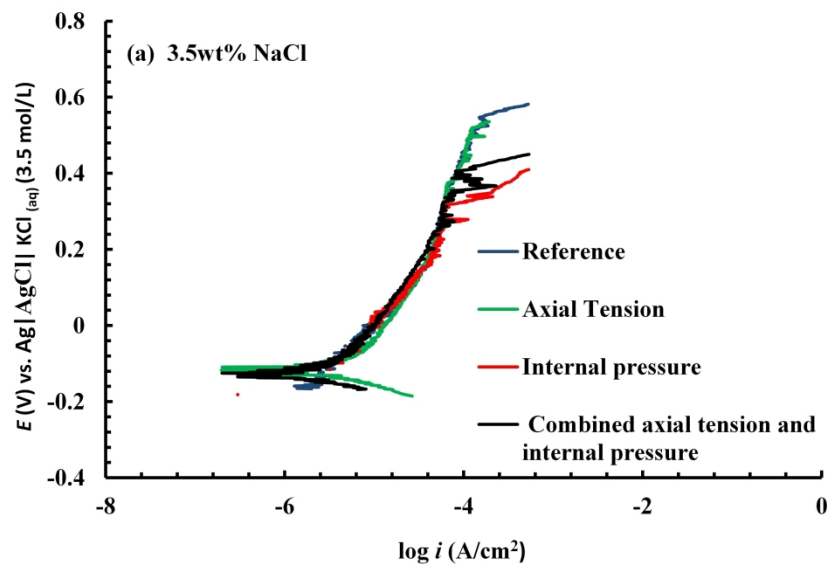
47 1046x1362mm (96 x 96 DPI)



44
45
46
47
48
49
50
51
52
53
54
55
56
57
58
59
60

Polarisation scan of SDSS for two nominally identical mini pipes subject to combined axial tension and internal pressure at 90 °C in (a) 3.5 wt% NaCl solution and (b) 3.5 wt% NaCl plus 100 ppmw ammonium bisulphite

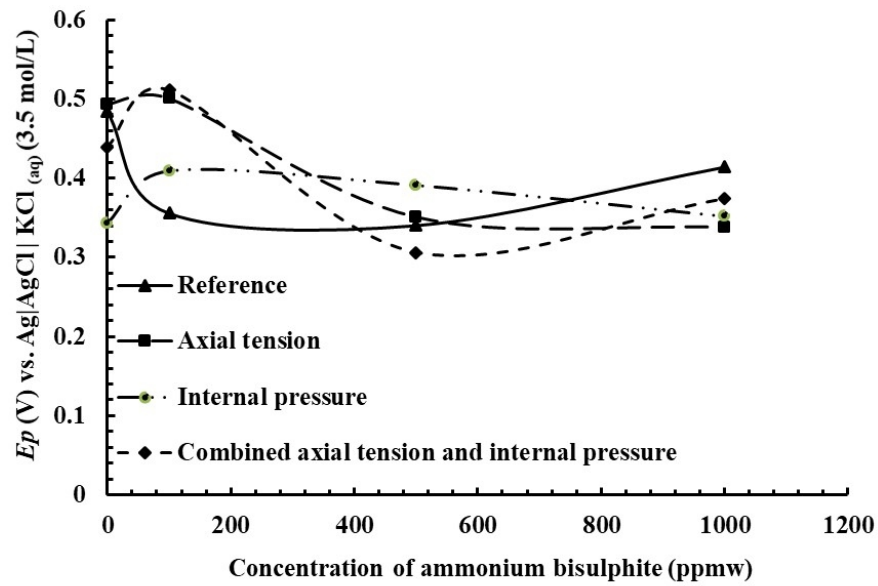
998x1322mm (96 x 96 DPI)



45 Effect of externally applied load on the polarisation scan of SDSS mini pipes exposed at 90 oC to 3.5 wt%
46 NaCl solutions (0 ppmw and 500 ppmw ammonium bisulphite).

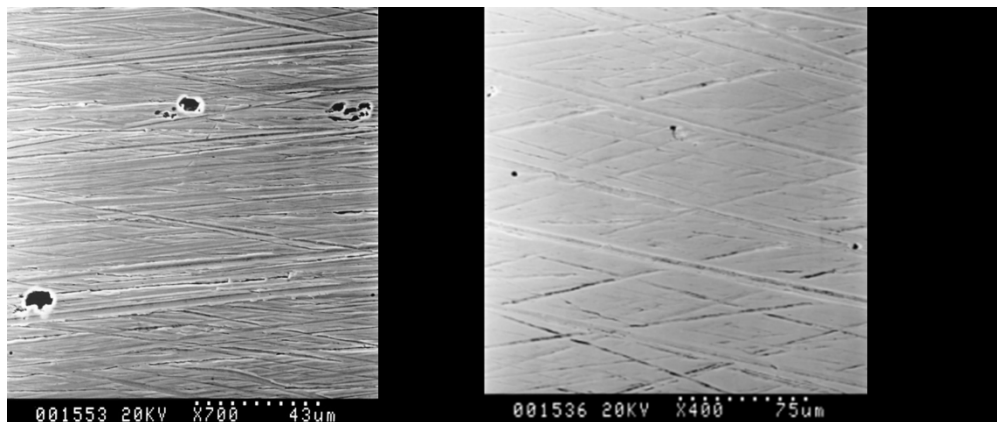
47 Figure 11 - The effect of external load and concentration of ammonium bisulphite in 3.5 wt% NaCl on the
48 pitting potential of SDSS at 90 oC

49
50 1034x1310mm (96 x 96 DPI)



The effect of external load and concentration of ammonium bisulphite in 3.5 wt% NaCl on the pitting potential of SDSS at 90 °C

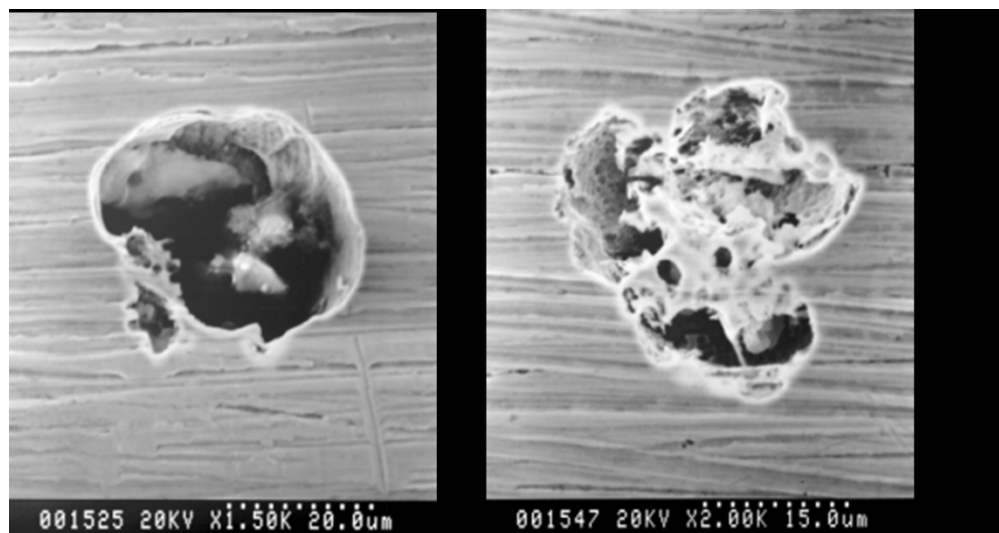
165x107mm (150 x 150 DPI)



Effect of ammonium bisulphite addition to 3.5 wt% NaCl at 90 oC on the initiation of pits on the surface of the 25Cr SDSS mini pipe in (a) 3.5 wt% NaCl and subject to axial load, and (b) 3.5 wt% NaCl plus 500 ppmw ammonium bisulphite subject to internal pressure

Note: The picture on the left is (a) and the right is (b)

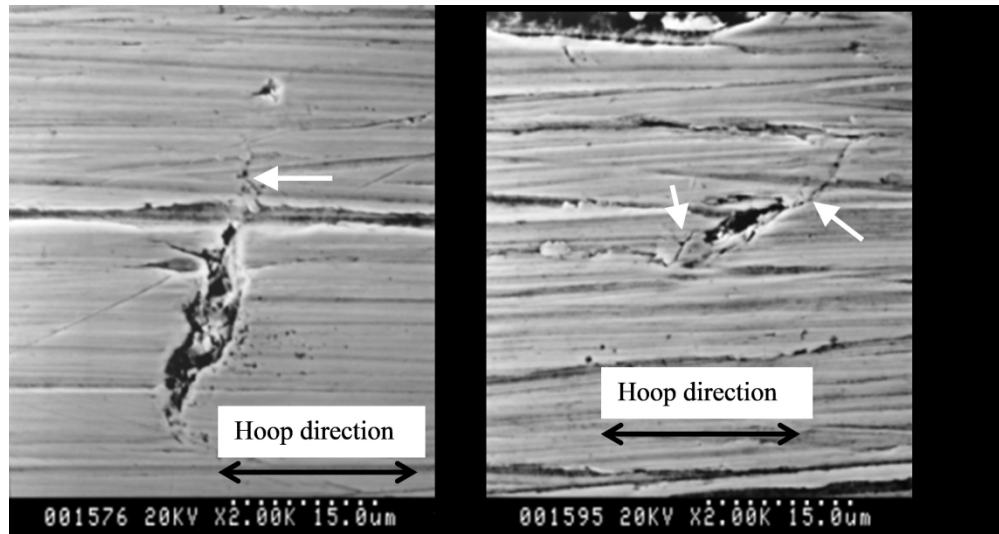
997x417mm (96 x 96 DPI)



Effect of ammonium bisulphite concentration in 3.5 wt% NaCl on the amount of deposits in pits on 25Cr SDSS pipes subjected to internal pressure and tested at 90 °C. (a) 3.5 wt% NaCl plus 100 ppmw ammonium bisulphite and (b) 3.5 wt% NaCl plus 1000 ppmw ammonium bisulphite

Note: The picture on the left is (a) and the right is (b)

997x527mm (96 x 96 DPI)



Typical crack initiation from pits on the surface of 25Cr SDSS mini pipe in 3.5wt% NaCl solutions plus different concentration of ammonium bisulphite. The white filled arrows indicate the cracks initiated from pits

Note: The picture on the left is (a) and the right is (b); (a) combined load (0 ppmw) and (b) combined load (500 ppmw)

997x527mm (96 x 96 DPI)